ARTICLE OPEN

Check for updates

Frequent copy number gain of *MCL1* is a therapeutic target for osteosarcoma

Satoshi Takagi[1], Mikako Nakajima[1,2], Sumie Koike[1], Miho Takami[1], Yoshiya Sugiura[3,4], Seiji Sakata[3,5,6], Satoko Baba[3,5,6], Ai Takemoto[1], Tianyi Huang[1,2], Yosuke Seto[1], Masanori Saito[7], Yuki Funauchi[7,8], Keisuke Ae[7], Kengo Takeuchi[3,5,6], Naoya Fujita[9] and Ryohei Katayama[1,2]✉

Osteosarcoma (OS) is a primary malignant bone tumor primarily affecting children and adolescents. The lack of progress in drug development for OS is partly due to unidentified actionable oncogenic drivers common to OS. In this study, we demonstrate that copy number gains of *MCL1* frequently occur in OS, leading to vulnerability to therapies based on Mcl-1 inhibitors. Fluorescence in situ hybridization analysis of 41 specimens revealed *MCL1* amplification in 46.3% of patients with OS. Genetic inhibition of *MCL1* induced significant apoptosis in *MCL1*-amplified OS cells, and the pharmacological efficacy of Mcl-1 inhibitors was correlated with *MCL1* copy numbers. Chromosome 1q21.2-3 region, where *MCL1* is located, contains multiple genes related to the IGF-1R/PI3K pathway, including *PIP5K1A, TARS2, OUTD7B*, and *ENSA*, which also showed increased copy numbers in *MCL1*-amplified OS cells. Furthermore, combining Mcl-1 inhibitors with IGF-1R inhibitors resulted in synergistic cell death by overcoming drug tolerance conferred by the activation of IGF signaling and suppressed tumor growth in *MCL1*-amplified OS xenograft models. These results suggest that genomic amplification of *MCL1* in the 1q21.2-3 region, which occurred in approximately half of OS patients, may serve as a predictive biomarker for the combination therapy with an Mcl-1 inhibitor and an IGF1R inhibitor.

Oncogene (2025) 44:794–804; https://doi.org/10.1038/s41388-024-03251-6

Graphical Abstract

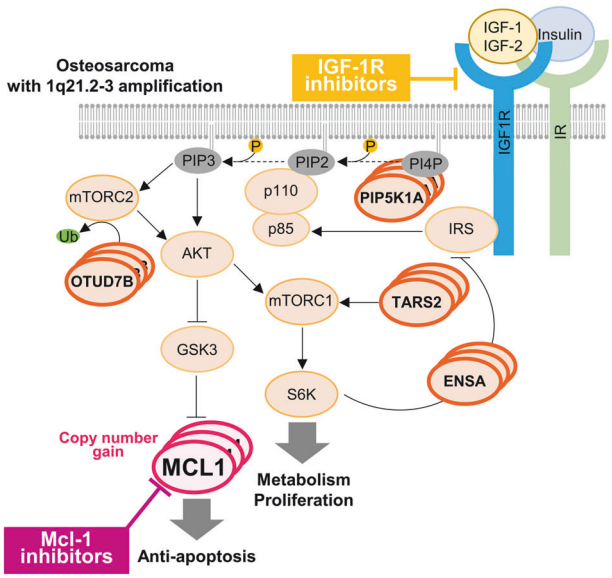

[1]Division of Experimental Chemotherapy, Cancer Chemotherapy Center, Japanese Foundation for Cancer Research (JFCR), Tokyo, Japan. [2]Department of Computational Biology and Medical Sciences, Graduate School of Frontier Science, The University of Tokyo, Tokyo, Japan. [3]Division of Pathology, Cancer Institute, JFCR, Tokyo, Japan. [4]Department of Pathology, Toho University Medical Center, Sakura Hospital, Sakura, Japan. [5]Department of Pathology, Cancer Institute Hospital, JFCR, Tokyo, Japan. [6]Pathology Project for Molecular Targets, Cancer Institute, JFCR, Tokyo, Japan. [7]Department of Orthopedic Oncology, Cancer Institute Hospital, JFCR, Tokyo, Japan. [8]Department of Orthopedic Surgery, Institute of Science Tokyo, Tokyo, Japan. [9]Cancer Chemotherapy Center, JFCR, Tokyo, Japan. ✉email: ryohei.katayama@jfcr.or.jp

Received: 29 November 2023 Revised: 26 November 2024 Accepted: 4 December 2024
Published online: 11 December 2024

INTRODUCTION

Osteosarcoma (OS) is the most common primary malignant bone tumor that predominantly occurs in children, adolescents, and young adults [1]. The treatment for OS that combines surgery with chemotherapy, which consists of a four-drug combination of doxorubicin (DOX), cisplatin (CDDP), high-dose methotrexate (MTX), and ifosfamide, was established in 1970s, and it is still used as a standard therapy [2]. The five-year overall survival rate of patients without distant metastases at the initial diagnosis has reached around 70% [3]; however, that of patients with metastatic or recurrent OS is only 20%–30% with poor prognosis and few effective treatments exist [4]. Recent clinical trials demonstrated the lack of activity of immune checkpoint inhibitors, including pembrolizumab, nivolumab, and ipilimumab, against OS [5], underscoring the critical need for new treatment strategies. While genetic alterations in TP53 and RB1 pathways occur frequently in OS, the commonly detected driver oncogene mutations and fusion genes that contribute to its pathogenesis have not been well-clarified yet [6, 7]. OS is characterized by widespread and recurrent copy number variations (CNVs) and structural variations (SVs), and these suggest that amplified or deleted genes could contribute as critical drivers of disease progression and malignancy in OS [6–8]. In fact, hierarchically stratified analyses of the Cancer Genome Atlas (TCGA) data indicate the different mechanisms of oncogenesis between mutation- and CNV-driven cancers [9]. Recently, a combination of whole-genome sequencing analysis from primary patient specimens with corresponding patient-derived xenograft (PDX) models demonstrates the utility of subclassification of patients with OS using CNV features to identify patient-specific vulnerabilities [10]. However, it remains unclear whether there are any OS-specific vulnerabilities that are broadly applicable to OS.

Apoptosis is programmed cell death executed by activating caspases, and there are two pathways for its induction: an intrinsic pathway mediated by mitochondria and an extrinsic pathway involving cell surface death receptors, such as Fas-R and TNFR1 [11]. The intrinsic pathway is regulated by Bcl-2 family proteins, which are classified into three categories: antiapoptotic proteins (Bcl-2, Bcl-xL, and Mcl-1), proapoptotic BH3-only proteins (Bad, Bik, and Bim), and effector proteins (Bak and Bax) [12]. Cancer cells frequently escape apoptosis by overexpressing antiapoptotic proteins, e.g., Mcl-1, this tendency has been reported in several cancers, including lung, breast, and gastrointestinal cancers, and sarcoma [13]. Mcl-1 expression is regulated by at multiple levels, including transcription by activation of the CREB transcription factor downstream of the PI3K/Akt pathway; translation by mTORC1 activation and subsequent 4E-BP1 phosphorylation; and protein stabilization by inhibition of GSK3-induced proteasome degradation [14]. BH3 mimetics are small molecular antagonists of antiapoptotic Bcl-2 members that function as competitive inhibitors by binding to a hydrophobic cleft [15]. In recent years, BH3 mimetics have been in active clinical trials, and a specific inhibitor of Bcl-2, venetoclax, has been approved for clinical use by the Food and Drug Administration (FDA) and the European Medicines Agency [12, 16, 17]. Nowadays, BH3 mimetics are the most promising approach for the inhibition of antiapoptotic Bcl-2 family proteins, and further ones are awaiting approval.

Insulin-like growth factor 1 receptor, IGF-1R, is a heterotetrameric transmembrane receptor tyrosine kinase whose natural ligands are IGF-1 and IGF-2; these contribute to cell proliferation, protein synthesis, and inhibition of apoptosis [18]. Ligand binding triggers the autophosphorylation of IGF-1R, which induces the interaction with intracellular adaptor proteins, such as IRS or SHC; these proteins activate downstream signaling via the PI3K/Akt/mTOR or Ras/Raf/ERK pathways [19]. The IGF-1R signaling pathway is important for bone growth; abnormalities in this pathway contribute to bone cancer progression [20, 21]. According to the genomic alterations between primary tumors and corresponding pulmonary metastatic sites by multiregional whole-exome and whole-genome sequencing in 10 patients with OS, the PI3K/Akt/mTOR pathway seems to be overactivated during early tumor development and pulmonary metastasis whereas RAS/MAPK pathway activation could rather play a role at later stages of pulmonary dissemination [22].

In this study, to explore the characteristic vulnerability in OS, molecular targeted drugs were screened against multiple OS cell lines and patient-derived cells. The molecular profiling of hit drugs revealed that Mcl-1 is important for OS cell survival and that approximately half of patients with OS have copy number gains of *MCL1*. The combination of Mcl-1 inhibitors with IGF-1R inhibitors induced synergistic cell death by overcoming the drug tolerance conferred by the activation of IGF signaling in vitro and suppressed *MCL1*-amplified OS tumor growth in vivo. Thus, our study demonstrated that the therapeutic strategy targeting Mcl-1 would be promising for OS with 1q21.2-3 amplification. Moreover, a FISH analysis that can detect *MCL1* gains in FFPE specimens from patients with OS was established to stratify patients eligible for this therapy.

RESULTS

Copy number amplification of *MCL1* occurs at a high frequency in OS, representing a potential vulnerability

To identify molecular targeted drugs that broadly suppress OS cell proliferation, drug screening was performed using our in-house inhibitor library of compounds with known targets [23]. Nine OS cell lines available from public cell banks and two OS patient-derived cell lines (PDCs) established in our laboratory were treated with an inhibitor library containing 92 molecular targeted drugs, and their effects on OS cell proliferation were evaluated (Supplementary Fig. S1A). A heat map comparison of cell viability identified that five drugs (obatoclax, tipifarnib, bortezomib, carfilzomib, and SN-38) exhibited a broad growth inhibition of OS cells. Obatoclax, which was originally identified as a pan-BH3 mimetic, exhibited a potent growth inhibitory effect on most of all OS cell lines; however, navitoclax, a dual BH3 mimetic of Bcl-2 and Bcl-xL, had little effects on OS growth (Supplementary Fig. S1B and S1C). Recently, it has been reported that obatoclax is not a true BH3 mimetic that induces mitochondrial permeabilization in a BAX/BAK-dependent manner, but its ability to kill primarily Mcl-1-dependent cells was demonstrated in the article [24]. To explore the potential dependence of OS on Mcl-1, CNVs of *MCL1* in OS cell lines were detected by the genomic DNA-targeting qPCR analysis. Notably, copy number gains of *MCL1* were observed at a high frequency of 45.5% (five out of 11 OS cell lines, Fig. 1A). Immunoblotting for Bcl-2 family proteins showed that Mcl-1 was broadly expressed in all OS cell lines except G-292; Bcl-xL was abundantly expressed, but Bcl-2 expression was below detection limits in many OS cells (Fig. 1B). *MCL1* amplification was also confirmed in NOS-10 and Sa-xeno-184 cells but not in Sa-xeno-147 and G-292 cells, using originally designed FISH probes (Fig. 1C), consistent with the qPCR results. Additionally, a copy number gain of *BCL2L1*, which encodes Bcl-xL, was observed in G-292 cells, where Mcl-1 expression was notably low.

To evaluate the contribution of Mcl-1 in OS cell survival, siRNAs specific for Bcl-2, Bcl-xL, or Mcl-1 were introduced into NOS-10 with *MCL1* amplification, Sa-xeno-147 without *MCL1* and *BCL2L1* amplification, and G-292 with *BCL2L1* amplification cells (Fig. 1D–I). Since the expression level of Bcl-2 protein was below the detection limit of immunoblot analysis, the knockdown efficacy of Bcl-2 in Sa-xeno-147 and G-292 cells was confirmed at the mRNA level by RT-qPCR (Supplementary Fig. S2A and S2B). The knockdown of Mcl-1 markedly increased the level of apoptotic marker, cleaved PARP, and Caspase-3/7 activity in NOS-10 cells. Although these trends were also observed in Sa-xeno-147 cells, the efficiency of apoptosis induction was much lower than in NOS-10 cells. In our interest, Bcl-xL knockdown increased cleaved PARP levels and Caspase-3/7 activity only in G-292 cells, indicating that

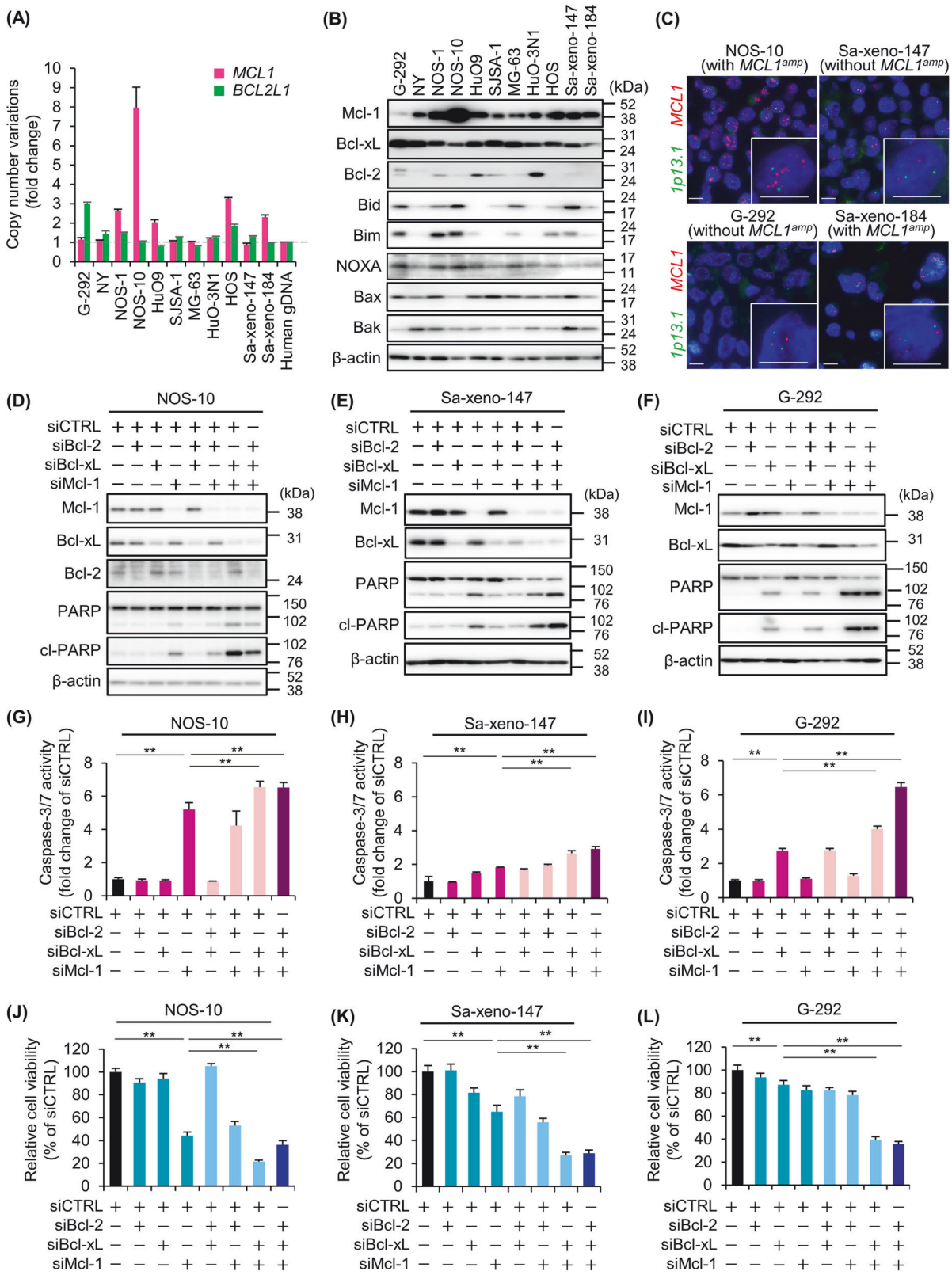

copy number gains of *BCL2L1* could also be a vulnerability in OS cells. The viability of all three OS cells was considerably reduced by the double knockdown of Mcl-1 and Bcl-xL (Fig. 1J–1L). These results indicate that Mcl-1 and Bcl-xL play important roles in OS cell survival and that copy number gains of either could be a potential molecular target in OS cells.

CNVs of *MCL1* reflect the sensitivity to Mcl-1 inhibitor in OS cells

To investigate the effect of pharmacological inhibition of antiapoptotic Bcl-2 family proteins on OS cell proliferation, we treated OS cells with five Bcl-2 family inhibitors (MIK665 and AZD5991 for Mcl-1; A-1331852 for Bcl-xL; venetoclax for Bcl-2;

Fig. 1 Copy number amplification of *MCL1* occurs at a high frequency in OS, representing a potential vulnerability. A The copy number variations (CNVs) of *MCL1* and *BCL2L1* in OS cells measured by qPCR. Each copy number is quantified relative to *LINE1* levels and represented as fold change. The human genomic DNA is used as a normal reference DNA. Data are shown as mean ± *SD* ($n = 3$). **B** Protein expression levels of Bcl-2 family proteins in OS cells. Each protein expression is detected using immunoblot with the indicated antibodies. **C** Detection of copy number gains of *MCL1* in OS cells by Fluorescence in situ hybridization (FISH) analysis. The ChromaTide TexasRed-12-dUTP targeting the human *MCL1* gene in 1q21.2 (red), and Fluorescein-12-dUTP targeting sequences in the chromosomal region 1p13.1 (green) are hybridized to cell blocks. Scale bars: 20 µm. **D**–**L** Effects of RNAi mediated gene knockdown of Mcl-1, Bcl-xL, or Bcl-2 in NOS-10, Sa-xeno-147, and G-292 cells. The knockdown efficacy is confirmed 24–48 h after siRNA treatment by the immunoblotting (**D**–**F**) and qPCR (Supplementary Fig. S2). Each protein expression is detected using immunoblot with the indicated antibodies. **G**–**I** Effects of siRNAs on the caspase-3/7 activity of OS cells. Caspase activities are measured using a Caspase-Glo 3/7 Assay reagent after 48 h of siRNA treatment. Data are shown as mean ± SD ($n = 4$). $^{**}p < 0.01$ as determined by Student's *t*-test. **J**–**L** Effects of siRNAs on OS cell viability. Cell viability is measured using a CellTiter-Glo Assay reagent after 48 h of siRNA treatment. Data are shown as mean ± SD ($n = 4$). $^{**}p < 0.01$ as determined by Student's *t*-test.

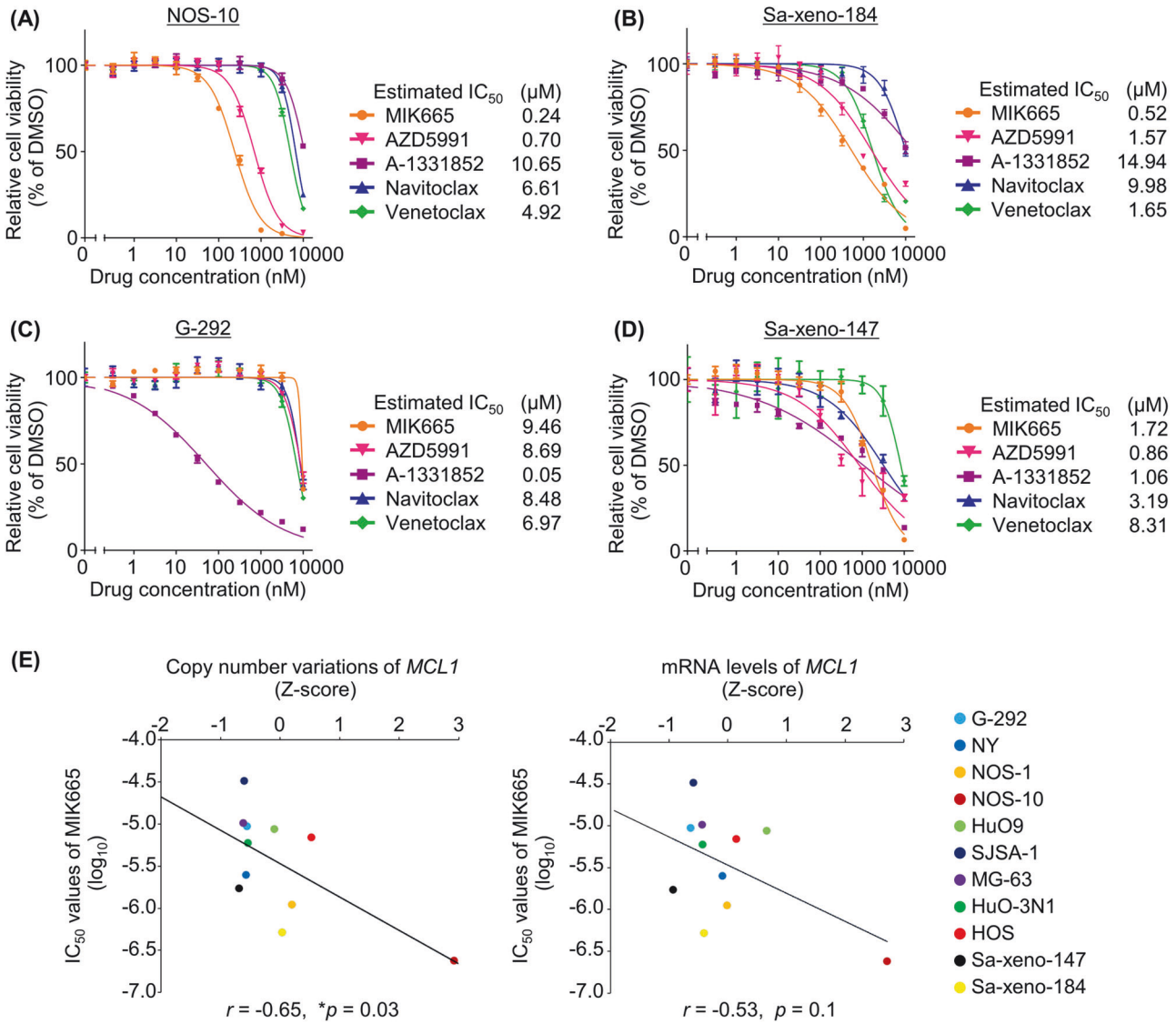

Fig. 2 Copy number variations of *MCL1* reflect the sensitivity to Mcl-1 inhibitor in OS cells. A–**D** The drug sensitivity of BH3 mimetics, including MIK665, AZD5991, A-1331852, navitoclax, and venetoclax are evaluated against NOS-10 (**A**), Sa-xeno-184 (**B**), G-292 (**C**), and Sa-xeno-147 (**D**) cells. Cell viability is measured using a CellTiter-Glo Assay reagent 72 h after drug treatment. All data are shown as means ± SD ($n = 3$). GraphPad Prism is used to calculate IC_{50} values and graphically display the data. **E** The Pearson's correlation analysis between the IC_{50} values of MIK665 and either copy number variations or mRNA levels of *MCL1* in 11 OS cell lines.

navitoclax for Bcl-2 and Bcl-xL) and found that NOS-10 and Sa-xeno-184 cells with copy number gains of *MCL1* were more sensitive to MIK665 and AZD5991 than the other compounds (Fig. 2A, B). G-292 cells with *BCL2L1* amplification were selectively sensitive to A-1331852 (Fig. 2C). Sa-xeno-147 cells were moderately sensitive to Mcl-1 and Bcl-xL inhibitors (Fig. 2D). Therefore, we performed a Pearson's correlation analysis between the IC_{50} values of MIK665 and the expression levels of *MCL1* in OS cell lines, to validate whether *MCL1* amplification is a biomarker for Mcl-1 dependency, and found that CNVs but not mRNA levels of *MCL1* reflect the drug sensitivity to MIK665 in OS cells (Fig. 2E). Consistent with the results of genetic knockdown of Bcl-2 family

proteins, the combination of A-1331852 with either MIK665 or AZD5991 dramatically reduced the viability of most of OS cell lines (Supplementary Fig. S3A–S3J), indicating that dual inhibition of Mcl-1 and Bcl-xL induces strong cytotoxicity in OS cells regardless the *MCL1* copy number status.

Various BH3 mimetics are currently being investigated for use in combination with standard therapy, and venetoclax, in combination with cytarabine or hypomethylating agents, had a significant clinical success in acute myeloid leukemia [15]. DOX, CDDP, MTX, and IFO are used as standard treatments for OS, and IFO is a prodrug alkylating agent that is metabolized and activated by hepatic cytochrome P450 in the body. Therefore, it was investigated whether DOX, CDDP, or MTX, in combination with Mcl-1 inhibitors, exhibits a synergistic growth inhibition of OS cells in vitro. Unfortunately, the IC_{50} values of DOX, CDDP, nor MTX were not reduced even in the presence of AZD5991 and A-1331852 (Supplementary Figure S3K–S3M), suggesting that standard chemotherapeutic agents for OS may not induce synergistic cytotoxic effects in the combination with Mcl-1 inhibitors.

The combination of Mcl-1 inhibitors enhances IGF-1R inhibitors-induced apoptosis by overcoming the drug tolerance conferred by IGF signaling activation in OS cells

To identify the suitable combination partner of Mcl-1 inhibitors for OS treatment, further drug screening was performed using our in-house inhibitor library (Supplementary Table1). It was found that Mcl-1 inhibitors sensitized OS cells to IGF-1R inhibitors, including OSI906, AEW541, and AZD3463, and significantly decreased their IC_{50} values (Fig. 3A–3F). Immunoblotting analysis confirmed that at least one of IGF-1R and IR is expressed in OS cell lines (Fig. 3G). The IGF-1R pathway has been implicated in the pathogenesis of bone and soft tissue sarcomas, including OS, Ewing sarcoma, rhabdomyosarcoma, and synovial sarcoma [25]. Clinically significant activity with partial responses in patients with OS has been also reported by a phase II study of a human monoclonal antibody to IGF1-R [26]. In our interest, several genes involved in the regulation of IGF1-R/PI3K/Akt/mTOR pathway, including *PIP5K1A*, the product of which is a upstream lipid kinase of PI3K predominantly responsible for the synthesis of PtdIns-4,5-P2 (PIP2), *TARS2*, the product of which activates mTORC1 in a threonine-dependent manner, *OUTD7B*, the product of which facilitates mTORC2 formation by removing polyubiquitin chains from GβL, and *ENSA*, the product of which modulates the feedback loops induced by sustained mTORC1/S6K activity, are located next to the *MCL1* locus 1q21.2-3 (Fig. 3H and Supplementary Fig. S4) [27–30] and copy number gains of these genes were also found in *MCL1*-amplified OS cell lines (Fig. 3I), suggesting that OS with *MCL1* amplification could readily activate downstream signaling pathways via IGF1-R. This result is consistent with the previous report that chromosome 1q21.2-3 region is frequently amplified in patients with OS [31]. Moreover, IGF-1/insulin reportedly induces Mcl-1 expression at multiple levels, including transcription by activating the CREB transcription factor located downstream of the PI3K/Akt pathway; translation by mTORC1 activation and subsequent 4E-BP1 phosphorylation; and protein stabilization by inhibiting GSK3-induced proteasome degradation [14, 32]. We also confirmed that Mcl-1 expression was immediately increased by the IGF-1 treatment in 3 hr and decreased by OSI906 treatment in NOS-10 cells (Supplementary Fig. S5A and S5B). Therefore, we next investigated the effect of IGF-1R pathway activation on the Mcl-1 inhibitors-induced apoptosis and found that MIK665- or AZD5991-induced apoptosis was negated by IGF-1 treatment, which was overcome in the presence of OSI906, a dual inhibitor of IGF-1R and IR (Fig. 3J, K). These results suggest that *MCL1*-amplified OS cells have a higher degree of activation of the PI3K/Akt/mTOR pathway, a downstream of IGF-1R and that the combination treatment of IGF-1R inhibitors with Mcl-1 inhibitors efficiently induces apoptosis in OS cells by overcoming the IGF signaling-mediated antiapoptotic effects.

The combination therapy of Mcl-1 inhibitors with OSI906 suppresses *MCL1*-amplified OS tumor growth in vivo

To evaluate the efficacy of combination therapy of MIK665 and OSI906, two murine xenograft models of OS with different copy numbers of *MCL1* were used in therapeutic experiments (Fig. 4A). In a NOS-10 (16 copies of *MCL1*) xenograft model, MIK665 suppressed the tumor growth and its antitumor effect was remarkably enhanced by combining with OSI906 (Fig. 4B). This trend was also observed in a NOS-1 (5 copies of *MCL1*) xenograft model, but the enhancement was more modest than in the NOS-10 model (Fig. 4C). Moreover, we also investigated the combination therapy of AZD5991 with OSI906 and found that combination of both also suppressed tumor growth in the NOS-10 xenograft model (Figs. 4D, E). These results indicate that combining Mcl-1 inhibitors with IGF-1R inhibitors could be a potential therapeutic intervention for *MCL1*-amplified OS.

Genomic copy number and protein expression of *MCL1* in patients with OS

To evaluate the copy number gains of *MCL1* in patients with OS, we performed FISH and immunohistochemical (IHC) analyses using tissue microarray consists of OS specimens. FISH analysis of specimens of patients with OS ($n = 41$) revealed that 14.6% ($n = 6$) and 31.7% ($n = 13$) had high- and low-level gain of *MCL1*, respectively (Fig. 5A, B). IHC staining also revealed high expression of Mcl-1 protein in specimens with *MCL1*-amplification in FISH analysis (Fig. 5C). These results indicated that *MCL1* copy number gains are detectable in FFPE specimens from patients with OS and could be used as a biomarker to predict the efficacy of the combination therapy.

A comprehensive analysis of CNVs of *MCL1* in pediatric patients with OS

A comprehensive analysis of CNVs in pediatric patients with OS was conducted using the TARGET OS datasets (Fig. 6). The results showed that the frequency of *MCL1* copy number gain was 70.4% (57 out of 81 patients), which is comparable to the frequency of 77.8% (63 out of 81 patients) observed for *MYC*, a gene known for its propensity for copy number amplification in younger OS patients. This suggests that *MCL1* amplification may be more prevalent in younger patients with OS.

DISCUSSION

In this study, we demonstrated that copy number gains of *MCL1* frequently occur in OS, leading to increased vulnerability to therapies based on Mcl-1 inhibitors (Fig. 7). To clarify the Mcl-1 dependency in OS cells, we utilized two structurally distinct Mcl-1 inhibitors, MIK665 and AZD5991, and found a negative correlation between *MCL1* copy numbers and sensitivity to MIK665, the more potent and specific inhibitor, with Pearson's r value of -0.65 ($^*p < 0.05$) in OS cell lines. The frequency of *MCL1* copy number gain was 45.5% in OS cell lines ($n = 11$) and 46.3% in FFPE specimens from patients with OS ($n = 41$), which is consistent with the previous report that chromosome 1q21.2-3 region, where *MCL1* is located, is frequently amplified in 48.3% of patients with OS ($n = 147$) [31]. In an analysis of the TARGET OS dataset, which comprises pediatric patients with OS ($n = 81$), the frequency of *MCL1* amplification was notably higher, at 70.4%. This study demonstrates that CNVs of *MCL1* in OS is a promising biomarker for predicting the efficacy of Mcl-1 inhibitor-based therapies and can be rapidly diagnosed by FISH.

A selective Bcl-xL inhibitor A-1331852 specifically reduced the viability of G-292 cells, which have a copy number gain of *BCL2L1*.

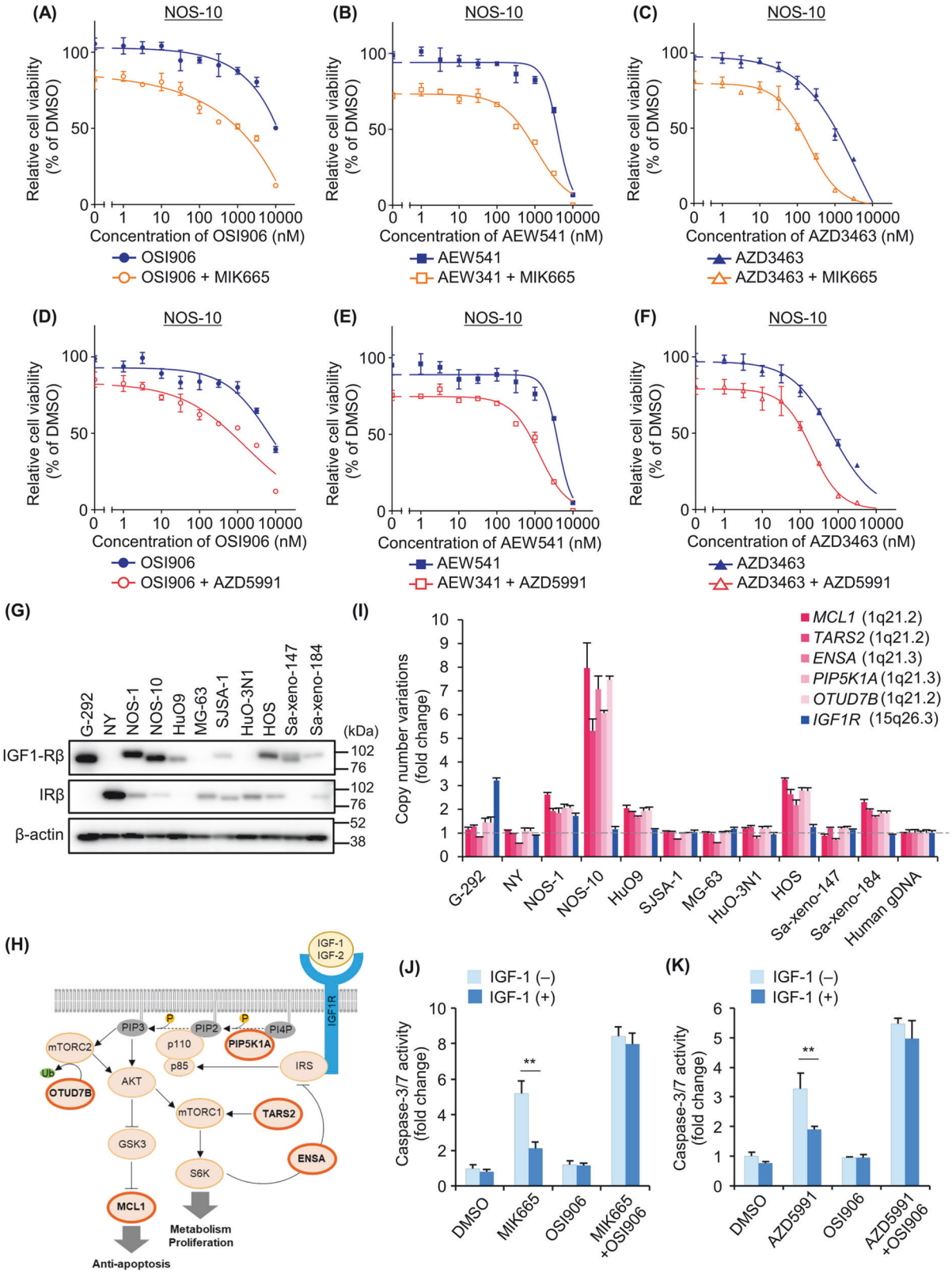

This result was surprising to us, since genetic inhibition experiments suggested that G-292 cells exhibited mutual substitution of antiapoptotic Bcl-2 family proteins. *BCL2L1* gene product is alternatively spliced to produce not only Bcl-xL but also Bcl-xS, an antagonistic isoform of Bcl-xL which can promote apoptosis. Bcl-xS can inhibit the function of Bcl-xL by forming heterodimers with Bcl-xL through the BH3 domain, or disrupting the VDAC2-Bak complex to cause the release of Bak and activation of MOMP [33]. If A-1331852 selectively interacts only with Bcl-xL, it could induce much potent apoptosis in OS cells with *BCL2L1* amplification by

Fig. 3 The combination of Mcl-1 inhibitors enhances IGF-1R inhibitors-induced apoptosis by overcoming the drug tolerance conferred by IGF signaling activation in OS cells. A–F Combination effects of 200 nM MIK665 or 500 nM AZD5991 with IGF-1R inhibitors, OSI906 (**A**, **D**), AEW541 (**B**, **E**), or AZD3463 (**C**, **F**) on NOS-10 cell viability. Cell viability is measured using CellTiter-Glo Assay reagent 72 h after drug treatment. All data are shown as mean ± *SD* ($n = 3$). GraphPad Prism is used to calculate IC_{50} values and graphically display the data. **G** Expression levels of IGF-1Rβ or IRβ proteins in OS cell lines. Each protein expression is detected using immunoblot with the indicated antibodies. **H** A schematic illustration showing the IGF-1R/PI3K/Akt/mTOR pathway and amplified molecules located on chromosome 1q21.2-3. Molecules for which copy number gains were observed in *MCL1*-amplified OS cells are shown in bold. **I** The CNVs of IGF-1R/PI3K/Akt/mTOR pathway-related genes located on chromosome 1q21.2-3, including *MCL1, TARS2, ENSA, PIP5K1A*, and *OTUD7B* in OS cell lines. *IGF1R* was measured as a negative control which located on chromosome 15q26.3. CNVs were measured by qPCR, and each copy number is quantified relative to *LINE1* levels and represented as fold change. The human genomic DNA is used as a normal reference DNA. Data are shown as mean ± *SD* ($n = 3$). Chromosomal localization of each gene is given in brackets. **J–K** The effect of IGF-1 treatment on Mcl-1 inhibitors-induced apoptosis in NOS-10 cells. NOS-10 cells are pretreated with 30 nM MIK665 (**J**) or 30 nM AZD5991 (K) in the presence or absence of 4 μM OSI906 for 30 min, and then treated with 40 ng/mL of IGF-1. Caspase activities are measured using a Caspase-Glo 3/7 Assay reagent after 24 h of IGF-1 treatment. Data are shown as mean ± SD ($n = 4$). $^{**}p < 0.01$ as determined by Student's *t*-test.

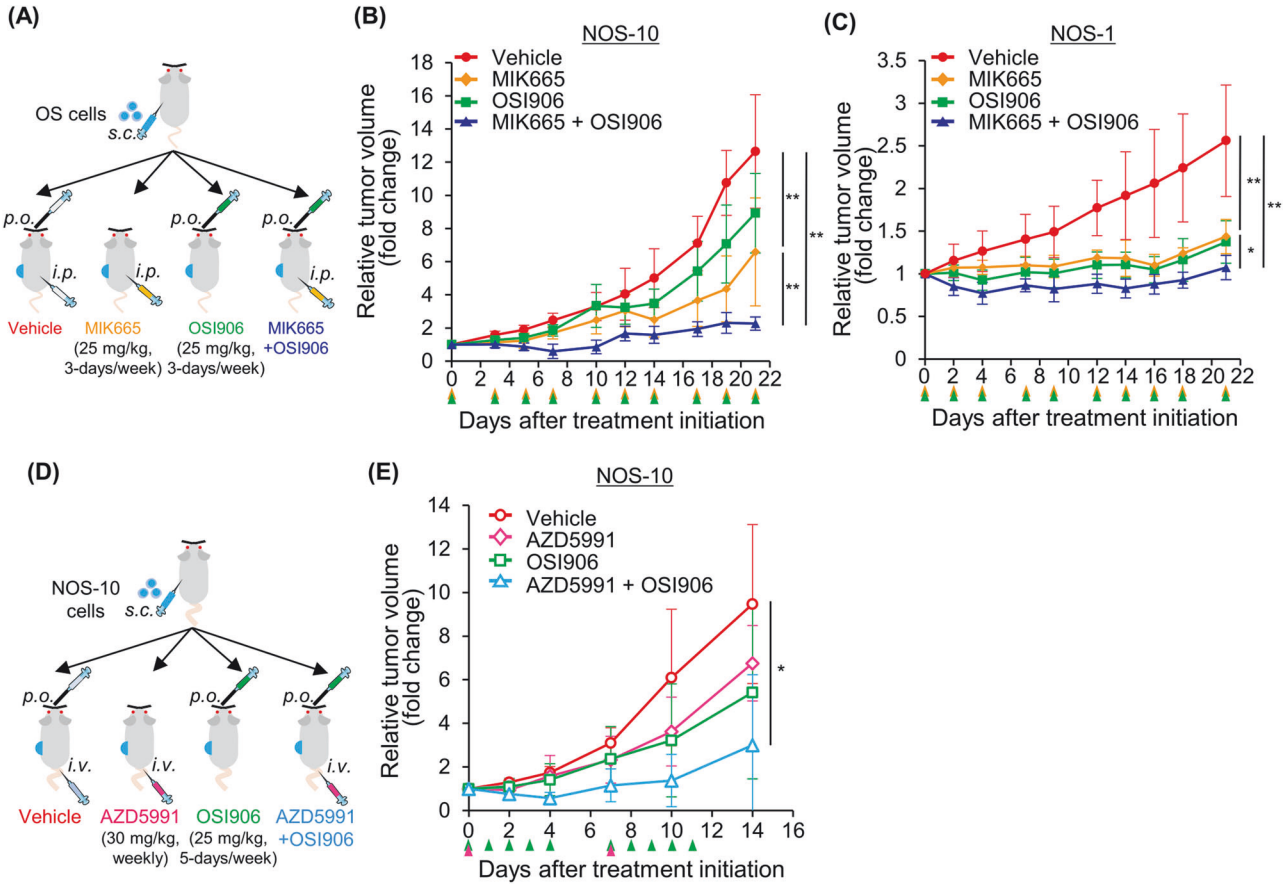

Fig. 4 The combination therapy of Mcl-1 inhibitors with OSI906 suppresses *MCL1*-amplified OS tumor growth in vivo. A Scheme of the combination therapy of MIK665 with OSI906 in vivo. **B**, **C** Relative tumor volume changes of NOS-10 (**B**) and NOS-1 (**C**) through the drug treatment. NOS-10 or NOS-1 cells are subcutaneously inoculated into immunodeficient SCID-beige mice (2.5×10^6 or 1×10^6 cells/mouse) and treated with 25 mg/kg of MIK665 intraperitoneally or 25 mg/kg of OSI906 orally three times a week. Arrowheads indicate timing of drug administration. All data are shown as mean ± *SD* ($n = 5$ or 6). **D** Scheme of the combination therapy of AZD5991 with OSI906 in vivo. **E** Relative tumor volume changes of NOS-10 through the drug treatment. NOS-10 cells are subcutaneously inoculated into SCID-beige mice (5×10^6 cells/mouse). AZD5991 and its vehicle control are intravenously administrated once a week. OSI906 and its vehicle control are orally administrated three times a week. Arrowheads indicate timing of drug administration. All data are shown as mean ± *SD* ($n = 5$). $^{**}p < 0.01$, $^{*}p < 0.05$ as determined by Mann–Whitney *U* test.

promoting Bcl-xS function. Further detailed analysis is required for OS with a copy number gain of *BCL2L1*.

The dual inhibition of Mcl-1 and Bcl-xL induces strong cytotoxicity in OS cells regardless the *MCL1* copy number status. Although we also investigated the effect of combination therapy of AZD5991 with A-1331852 in the NOS-10-xenograft model, we could not find the appropriate therapeutic window due to the toxicity. The strong cytotoxicity induced by the dual inhibition of Mcl-1 and Bcl-xL has been reported in other types of cancers and occurred regardless of driver gene mutations or cellular origin, suggesting that it is a general apoptosis caused by the simultaneous inhibition of all major antiapoptotic Bcl-2 family members in cells [34].

Chromosome 1q21.2-3 region contains several genes that enhance the IGF-1R/PI3K/Akt/mTOR pathway, including *PIP5K1A, TARS2, OUTD7B*, and *ENSA*, with increased copy numbers observed in *MCL1*-amplified OS cells. Chromosome 1q frequently exhibits structural and numerical abnormalities in various cancers, including breast and lung cancer. According to the COSMIC database, copy

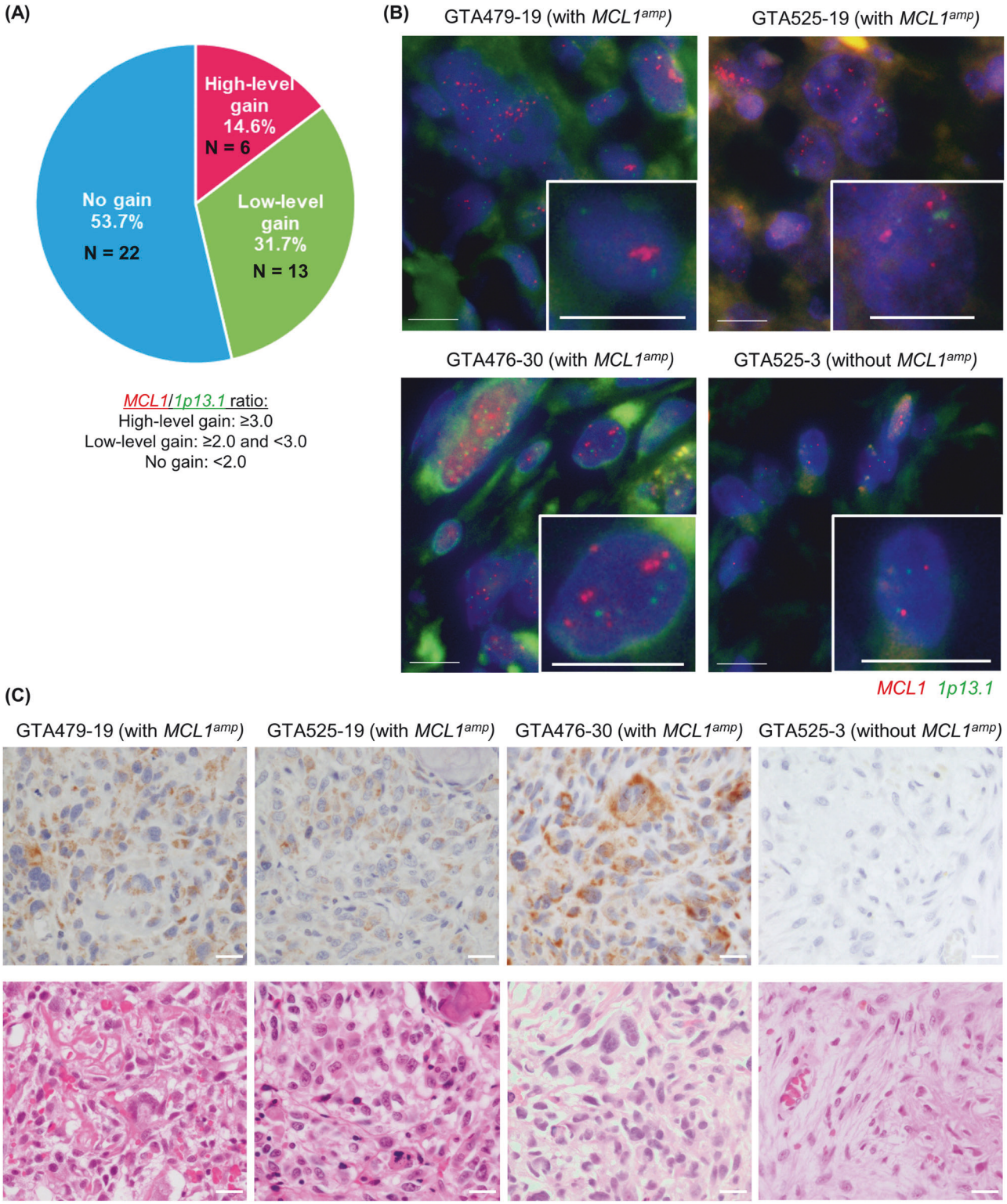

Fig. 5 Genomic copy number and protein expression of *MCL1* in patients with OS. A Copy number gain of *MCL1* in 41 patients with OS. The ratio of *MCL1* to *1p13.1* in 41 FFPE specimens from patients with OS was measured by the *MCL1* FISH analysis. *MCL1* gene gain is defined as *MCL1/1p13.1* ratio ≥ 2.0, with high-level gain as *MCL1/1p13.1* ratio ≥ 3.0 and low-level gain as *MCL1/1p13.1* ratio ≥ 2.0 and < 3.0. **B**, **C** Examples of *MCL1* FISH (**B**) and immunohistochemical (IHC, **C**) analyses in the specimens of patients with OS. Three specimens (GTA479-19, GTA525-19, and GTA476-30) defined as *MCL1*-amplified and one specimen (GTA525-3) defined as no gain is represented. An anti-Mcl-1 monoclonal antibody (CST, Cat#39224) is used for IHC staining (**C**). Scale bars: 20 μm.

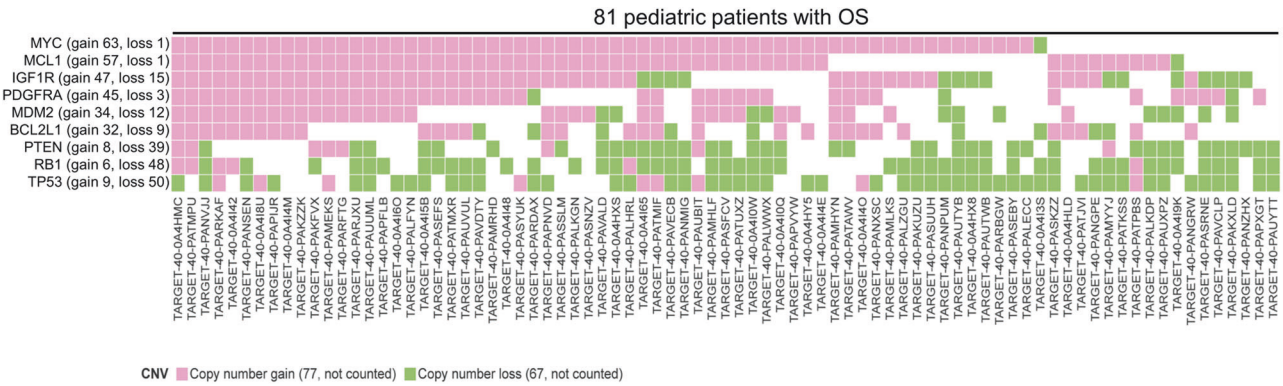

Fig. 6 Copy number variations of genes in the TARGET OS dataset. Copy number variations of *MYC* (gain 63, loss 1), *MCL1* (gain 57, loss 1), *IGF1R* (gain 47, loss 15), *PDGFRA* (gain 45, loss 3), *MDM2* (gain 34, loss 12), *BCL2L1* (gain 32, loss 9), *PTEN* (gain 8, loss 39), *RB1* (gain 6, loss 48), and *TP53* (gain 9, loss 50) genes in 81 pediatric patients with osteosarcoma in the TARGER dataset.

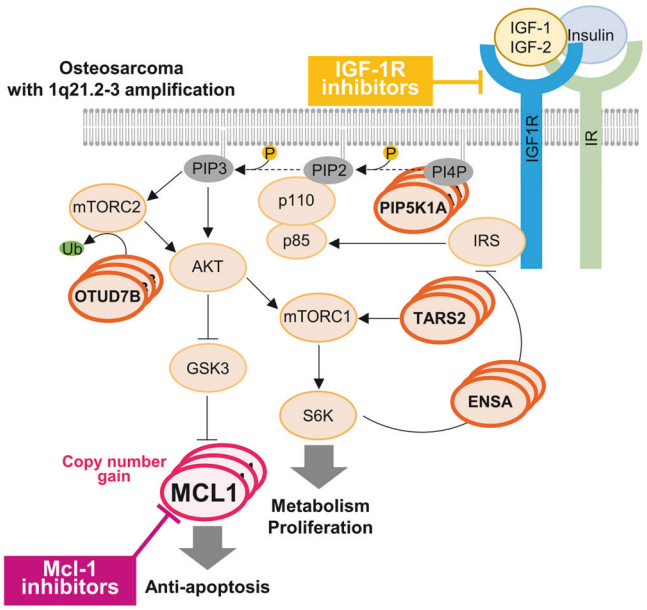

Fig. 7 Copy number gains of *MCL1* frequently occur in OS, leading to increased vulnerability to therapies based on Mcl-1 inhibitors. A schematic illustration of potential therapeutic intervention for OS with 1q21.2-3 amplification based on the combination of Mcl-1 inhibitors with IGF-1R inhibitors. Molecules for which copy number gains were observed in *MCL1*-amplified OS cells are shown in bold.

number gains of *PIP5K1A* are reported in over 60% of breast cancer patients, predominantly in invasive breast carcinoma [35]. Additionally, other genes located on chromosome 1q, such as *PI4KB, PI3KC2B*, and *AKT3*, which are involved in phosphoinositide signaling, are also amplified in a subset of breast cancers [36]. Furthermore, copy number gains of *ENSA* have been reported in 57.6% of triple-negative breast cancer cases in the TCGA database and are known to promote tumor progression through cholesterol biosynthesis [37]. These data suggest that OS with 1q21.2-3 amplification shares structural and numerical chromosomal abnormalities similar to those found in certain breast cancers, collectively enhancing Mcl-1-dependent evasion of programmed cell death.

Clinical trials targeting IGF-1R currently include OSI906 for moderate to severe thyroid eye disease and ganitumab, an anti-IGF-1R monoclonal antibody, for metastatic Ewing sarcoma. In contrast, several clinical trials of Mcl-1 inhibitors have been conducted in hematologic and solid tumors, but with limited efficacy, particularly in patients with solid tumors. Additionally, Mcl-1 prevents cell death and regulates fatty acid oxidation in cardiomyocytes [38], there is a potential risk of cardiotoxicity associated with long-term inhibition of Mcl-1. Recently, BRD-810, a more potent Mcl-1 inhibitor with a shorter half-life, has shown promise in targeting cancer cells while sparing cardiomyocytes in preclinical models [39]. Such next generation of Mcl-1 inhibitors, combined with IGF-1R inhibitors and pre-stratification of patients based on *MCL1* copy numbers, may represent a novel therapeutic strategy for OS.

A limitation of this study is that the correlation between the prognosis of patients with OS and the scores of *MCL1* FISH or IHC were not verified. The decalcification process, which is required for bone tissue analysis, damaged the FFPE samples, making it impossible to evaluate staining levels in some of the initially planned samples. Therefore, no large-scale analysis of the correlation between *MCL1* amplification and prognosis in patients with OS was performed. We were also unable to determine a threshold for how much copy number gains of *MCL1* would be considered an indication for this combination therapy in vivo. Additionally, the amplification of both chromosome 8q24.21, where *MYC* is located, and 15q26.3, where *IGF1R* is located, is also frequently observed in younger patients with OS [8, 31], and c-Myc-mediated upregulation of Mcl-1 were reported in many cancer types [13] suggesting that therapeutic strategies targeting Mcl-1 might be extended to OS without *MCL1* amplification. Indeed, one of our established PDCs, Sa-xeno-147, has more than 100 copies of *MYC* (Supplementary Fig. S6) and tends to be relatively sensitive to Mcl-1 inhibitors, we would like to reveal these aspects in future studies.

In conclusion, our results indicated that combining Mcl-1 inhibitors with IGF-1R inhibitors would be a novel therapeutic option for advanced OS with *MCL1* amplification and that the copy number gains in *MCL1* would be a predictive biomarker for efficacy of this combination therapy.

MATERIALS AND METHODS

Cell lines

Human OS cell lines MG-63 (RRID: CVCL_0426), HOS (RRID: CVCL_0312), and SJSA-1 (RRID: CVCL_1697) were purchased from ATCC, NOS-10 (RRID: CVCL_4663) and NOS-1 (RRID: CVCL_1610) from RIKEN Bioresource Research Center; and NY (RRID: CVCL_1613), HuO9 (RRID: CVCL_1298), HuO-3N1 (RRID: CVCL_1297), and G-292 clone A141B1 (G-292, RRID: CVCL_2909) from JCRB Cell Bank. Sa-xeno-147 and Sa-xeno-184 cell lines established from clinical specimens of patients with osteosarcoma at JFCR Hospital were determined to be similar to the clinical sample and the primary culture via STR analysis [40]. Informed consent was obtained from all the patients and the study was conducted in accordance with the Declaration of Helsinki and with the approval of the Institutional Review Board of JFCR (IRB number: 2013-1092) [41]. Details of cell culture are described in the Supplementary Materials and Methods.

Animal procedures

All animal procedures were performed in accordance with relevant guidelines and regulations, according to the protocol approved by the Committee for the Use and Care of Experimental Animals of JFCR (protocol number: 10-01-22). Five- to six-week-old female SCID-beige (CB17.Cg-PrkdcscidLystbg-J/CrlCrlj) mice were purchased from Charles River Laboratories, Inc. NOS-10 or NOS-1 cells are subcutaneously inoculated into left flank of SCID-beige mice. When the average tumor volume reached approximately 50 mm^3, the mice were randomized into four groups. Each group was treated with vehicle, MIK665 intraperitoneally, or OSI906 orally three times a week. For the combination therapy of AZD5991 with OSI906, AZD5991 was intravenously administrated once a week and OSI906 is orally administrated five times a week. The experiments were independently repeated twice.

MCL1 FISH analysis

MCL1 gene copy number status was examined on the tissue microarray or cell blocks of OS cell lines determined using in-house probes made from BAC clones (the exact clone names are available upon request), which contained ChromaTide TexasRed-12-dUTP (Thermo Fisher Science) targeting the human *MCL1* gene in 1q21.2 and Fluorescein-12-dUTP (Roche) targeting sequences in the chromosomal region 1p13.1. The images were captured using an Olympus BX51 fluorescence microscope equipped with a charge-coupled device camera (DP71; Olympus, Tokyo, Japan). *MCL1* gene gain was defined as MCL1/1p13.1 ratio ≥ 2.0, with high-level gain as ≥ 3.0 and low-level gain as ≥ 2.0 and < 3.0.

Immunoblot analysis

Cells were harvested using a cell scraper, lysed in an SDS-lysis buffer [100 mM Tris-HCl (pH 7.5), 10% glycerol, 1% SDS], and boiled for 10 min. Protein concentrations were measured using a Pierce™ BCA Protein Assay Kit (Thermo Fisher) after centrifugation at 20,000 × g for 10 min. Equal amounts of cell lysates were electrophoresed in SDS-polyacrylamide gel. The proteins were transferred to polyvinylidene difluoride membranes and immunoblotted with antibodies listed in the Supplementary Table 2. HRP-conjugated anti-mouse or rabbit IgG and a SuperSignal West Femto Maximum Sensitivity Substrate (Thermo Fisher Scientific) were used for detection by an AI600 image analyzer (GE Healthcare). In some experiments, cells were resuspended in an NP-40 lysis buffer [20 mM Tris, 150 mM NaCl, 1% Nonidet P-40, 10% glycerol, 1 mM EDTA, 1 mM EGTA, and protease and phosphatase inhibitors]. For the detection of NOXA, the transferred membrane was cross-linked with 0.4% paraformaldehyde-PBS solution for 30 min before blocking the membrane. The experiments were independently repeated thrice.

Quantitative PCR

Complementary DNAs and genomic DNAs were prepared with ReverTra Ace qPCR RT Master Mix (TOYOBO) and DNeasy Blood & Tissue Kits (QIAGEN) respectively, following the manufacturer's protocols. Quantitative real-time polymerase chain reaction (qPCR) was performed using FastStart Essential DNA Green Master (Roche) and Light Cycler 96 (Roche) by the ΔΔCt method. The levels of *GAPDH* and the repetitive sequence element *LINE1* were used to calculate gene expressions and DNA copy numbers, respectively. The human genomic DNA (PROMEGA) was used as a template in the positive control for PCRs. Primers used in this study were listed in the Supplementary Table 3 [13, 42].

Inhibitor library screening

Cells were seeded at a density of 2000 cells/well in 96-well plates (Greiner) and cultured for 24 h. After 72 h of incubation with an original panel of inhibitor library, the cells were conducted for cell viability assay as detailed in the Supplemental Materials and Methods. The average values of two independent experiments were graphically displayed as a heat map using ComplexHeatmap version 2.4.3 (R version 4.0.2). The experiments were independently repeated twice. Screening results for single and combined agents are available in the Supplementary Table 1.

Statistical analysis

The Student's *t*-test was used to determine the statistical significance of the results of the in vitro experiments. The mouse analysis was compared using the Mann–Whitney *U* test. Significant *p* values are shown as $^{*}p < 0.05$ and $^{**}p < 0.01$. All statistical tests were two-sided. The Pearson's correlation coefficient (*r*) was used to measure a linear correlation between IC_{50} values of MIK665 and expression levels of *MCL1*.

DATA AVAILABILITY

The materials and data obtained in this study will be available upon reasonable request after the completion of a material transfer agreement.

REFERENCES

1. Kansara M, Teng MW, Smyth MJ, Thomas DM. Translational biology of osteosarcoma. Nat Rev Cancer. 2014;14:722–35.
2. Link MP, Goorin AM, Miser AW, Green AA, Pratt CB, Belasco JB, et al. The effect of adjuvant chemotherapy on relapse-free survival in patients with osteosarcoma of the extremity. N Engl J Med. 1986;314:1600–6.
3. Iwamoto Y, Tanaka K, Isu K, Kawai A, Tatezaki S, Ishii T, et al. Multiinstitutional phase II study of neoadjuvant chemotherapy for osteosarcoma (NECO study) in Japan: NECO-93J and NECO-95J. J Orthop Sci. 2009;14:397–404.
4. Huang X, Zhao J, Bai J, Shen H, Zhang B, Deng L, et al. Risk and clinicopathological features of osteosarcoma metastasis to the lung: A population-based study. J Bone Oncol. 2019;16:100230.
5. Tawbi HA, Burgess M, Bolejack V, Van Tine BA, Schuetze SM, Hu J, et al. Pembrolizumab in advanced soft-tissue sarcoma and bone sarcoma (SARC028): a multicentre, two-cohort, single-arm, open-label, phase 2 trial. Lancet Oncol. 2017;18:1493–501.
6. Chen X, Bahrami A, Pappo A, Easton J, Dalton J, Hedlund E, et al. Recurrent somatic structural variations contribute to tumorigenesis in pediatric osteosarcoma. Cell Rep. 2014;7:104–12.
7. Perry JA, Kiezun A, Tonzi P, Van Allen EM, Carter SL, Baca SC, et al. Complementary genomic approaches highlight the PI3K/mTOR pathway as a common vulnerability in osteosarcoma. Proc Natl Acad Sci USA. 2014;111:E5564–73.
8. Behjati S, Tarpey PS, Haase K, Ye H, Young MD, Alexandrov LB, et al. Recurrent mutation of IGF signalling genes and distinct patterns of genomic rearrangement in osteosarcoma. Nat Commun. 2017;8:15936.
9. Ciriello G, Miller ML, Aksoy BA, Senbabaoglu Y, Schultz N, Sander C. Emerging landscape of oncogenic signatures across human cancers. Nat Genet. 2013;45:1127–33.
10. Sayles LC, Breese MR, Koehne AL, Leung SG, Lee AG, Liu HY, et al. Genome-Informed Targeted Therapy for Osteosarcoma. Cancer Discov. 2019;9:46–63.
11. Danial NN, Korsmeyer SJ. Cell death: critical control points. Cell. 2004;116:205–19.
12. Lessene G, Czabotar PE, Colman PM. BCL-2 family antagonists for cancer therapy. Nat Rev Drug Discov. 2008;7:989–1000.
13. Beroukhim R, Mermel CH, Porter D, Wei G, Raychaudhuri S, Donovan J, et al. The landscape of somatic copy-number alteration across human cancers. Nature. 2010;463:899–905.
14. Hsieh AC, Costa M, Zollo O, Davis C, Feldman ME, Testa JR, et al. Genetic dissection of the oncogenic mTOR pathway reveals druggable addiction to translational control via 4EBP-eIF4E. Cancer Cell. 2010;17:249–61.
15. Parry N, Wheadon H, Copland M. The application of BH3 mimetics in myeloid leukemias. Cell Death Dis. 2021;12:222.
16. Liu T, Lam V, Thieme E, Sun D, Wang X, Xu F, et al. Pharmacologic Targeting of Mcl-1 Induces Mitochondrial Dysfunction and Apoptosis in B-Cell Lymphoma Cells in a TP53- and BAX-Dependent Manner. Clin Cancer Res. 2021;27:4910–22.
17. Leverson JD, Phillips DC, Mitten MJ, Boghaert ER, Diaz D, Tahir SK, et al. Exploiting selective BCL-2 family inhibitors to dissect cell survival dependencies and define improved strategies for cancer therapy. Sci Transl Med. 2015;7:279ra240.
18. Ekyalongo RC, Yee D. Revisiting the IGF-1R as a breast cancer target. NPJ Precis Oncol. 2017;1:14.
19. Iams WT, Lovly CM. Molecular Pathways: Clinical Applications and Future Direction of Insulin-like Growth Factor-1 Receptor Pathway Blockade. Clin Cancer Res. 2015;21:4270–7.
20. Kuijjer ML, Peterse EF, van den Akker BE, Briaire-de Bruijn IH, Serra M, Meza-Zepeda LA, et al. IR/IGF1R signaling as potential target for treatment of high-grade osteosarcoma. BMC cancer. 2013;13:245.
21. Rikhof B, de Jong S, Suurmeijer AJ, Meijer C, van der Graaf WT. The insulin-like growth factor system and sarcomas. J Pathol. 2009;217:469–82.
22. Wang D, Niu X, Wang Z, Song CL, Huang Z, Chen KN, et al. Multiregion Sequencing Reveals the Genetic Heterogeneity and Evolutionary History of Osteosarcoma and Matched Pulmonary Metastases. Cancer Res. 2019;79:7–20.
23. Shimizu Y, Okada K, Adachi J, Abe Y, Narumi R, Uchibori K, et al. GSK3 inhibition circumvents and overcomes acquired lorlatinib resistance in ALK-rearranged non-small-cell lung cancer. NPJ Precis Oncol. 2022;6:16.

24. Villalobos-Ortiz M, Ryan J, Mashaka TN, Opferman JT, Letai A. BH3 profiling discriminates on-target small molecule BH3 mimetics from putative mimetics. Cell Death Differ. 2020;27:999–1007.
25. Maki RG. Small is beautiful: insulin-like growth factors and their role in growth, development, and cancer. J Clin Oncol. 2010;28:4985–95.
26. Pappo AS, Vassal G, Crowley JJ, Bolejack V, Hogendoorn PC, Chugh R, et al. A phase 2 trial of R1507, a monoclonal antibody to the insulin-like growth factor-1 receptor (IGF-1R), in patients with recurrent or refractory rhabdomyosarcoma, osteosarcoma, synovial sarcoma, and other soft tissue sarcomas: results of a Sarcoma Alliance for Research Through Collaboration study. Cancer. 2014;120:2448–56.
27. Kim SH, Choi JH, Wang P, Go CD, Hesketh GG, Gingras AC, et al. Mitochondrial Threonyl-tRNA Synthetase TARS2 Is Required for Threonine-Sensitive mTORC1 Activation. Mol Cell. 2021;81:398–407.e394.
28. Sanz-Castillo B, Hurtado B, Vara-Ciruelos D, El Bakkali A, Hermida D, Salvador-Barbero B, et al. The MASTL/PP2A cell cycle kinase-phosphatase module restrains PI3K-Akt activity in an mTORC1-dependent manner. Embo j. 2023;42:e110833.
29. Hu J, Yuan Q, Kang X, Qin Y, Li L, Ha Y, et al. Resolution of structure of PIP5K1A reveals molecular mechanism for its regulation by dimerization and dishevelled. Nat Commun. 2015;6:8205.
30. Wang B, Jie Z, Joo D, Ordureau A, Liu P, Gan W, et al. TRAF2 and OTUD7B govern a ubiquitin-dependent switch that regulates mTORC2 signalling. Nature. 2017;545:365–9.
31. Taylor AM, Sun JM, Yu A, Voicu H, Shen J, Barkauskas DA, et al. Integrated DNA Copy Number and Expression Profiling Identifies IGF1R as a Prognostic Biomarker in Pediatric Osteosarcoma. Int J Mol Sci. 2022;23:8036.
32. Maurer U, Charvet C, Wagman AS, Dejardin E, Green DR. Glycogen synthase kinase-3 regulates mitochondrial outer membrane permeabilization and apoptosis by destabilization of MCL-1. Mol Cell. 2006;21:749–60.
33. Dou Z, Zhao D, Chen X, Xu C, Jin X, Zhang X, et al. Aberrant Bcl-x splicing in cancer: from molecular mechanism to therapeutic modulation. J Exp Clin Cancer Res. 2021;40:194.
34. Mukherjee N, Skees J, Todd KJ, West DA, Lambert KA, Robinson WA, et al. MCL1 inhibitors S63845/MIK665 plus Navitoclax synergistically kill difficult-to-treat melanoma cells. Cell Death Dis. 2020;11:443.
35. Yin M, Wang Y. The role of PIP5K1A in cancer development and progression. Med Oncol. 2022;39:151.
36. Waugh MG. Amplification of Chromosome 1q Genes Encoding the Phosphoinositide Signalling Enzymes PI4KB, AKT3, PIP5K1A and PI3KC2B in Breast Cancer. J Cancer. 2014;5:790–6.
37. Chen YY, Ge JY, Zhu SY, Shao ZM, Yu KD. Copy number amplification of ENSA promotes the progression of triple-negative breast cancer via cholesterol biosynthesis. Nat Commun. 2022;13:791.
38. Wright T, Turnis ME, Grace CR, Li X, Brakefield LA, Wang YD, et al. Anti-apoptotic MCL-1 promotes long-chain fatty acid oxidation through interaction with ACSL1. Mol Cell. 2024;84:1338–53.e1338.
39. Rauh U, Wei G, Serrano-Wu M, Kosmidis G, Kaulfuss S, Siegel F, et al. BRD-810 is a highly selective MCL1 inhibitor with optimized in vivo clearance and robust efficacy in solid and hematological tumor models. Nat. Cancer 2024;5:1479–93.
40. Takemoto A, Takagi S, Ukaji T, Gyobu N, Kakino M, Takami M, et al. Targeting Podoplanin for the Treatment of Osteosarcoma. Clin Cancer Res. 2022;28:2633–45.
41. Takagi S, Sasaki Y, Koike S, Takemoto A, Seto Y, Haraguchi M, et al. Platelet-derived lysophosphatidic acid mediated LPAR1 activation as a therapeutic target for osteosarcoma metastasis. Oncogene. 2021;40:5548–58.
42. Ariyasu R, Nishikawa S, Uchibori K, Oh-Hara T, Yoshizawa T, Dotsu Y, et al. High ratio of T790M to EGFR activating mutations correlate with the osimertinib response in non-small-cell lung cancer. Lung Cancer. 2018;117:1–6.

ACKNOWLEDGEMENTS

We thank Ms. Harumi Shibata, Mr. Tokuichi Kawaguchi, Dr. Minoru Sugawara, and Dr. Seiichi Matsumoto from JFCR for their technical assistance and advice.

AUTHOR CONTRIBUTIONS

ST and RK designed the study, supervised experiments, and wrote the manuscript. MN, SK, MT, and TH performed in vitro experiments. ST and AT performed in vivo experiments. YSugiura, SS, SB, and KT performed FISH and IHC analyses. ST and YSeto performed data analyses. MS, YF, and KA identified patients and obtained clinical samples. NF supervised in vitro and in vivo experiments. All authors reviewed and edited the manuscript.

FUNDING

This study was supported in part by JSPS KAKENHI grant number JP19K22572, JP23H02754 (to S. Takagi), JP22H02906 (to N. Fujita), and JP22K18383 (to R. Katayama). This study was also supported in part by Japan Agency for Medical Research and Development (AMED) grant number JP22cm0106286, JP24ama221220 (to S. Takagi), JP24ama221210, JP24ama221201 (to R. Katayama), and the grants from Nippon Foundation and Takeda Science Foundation (to N. Fujita).

COMPETING INTERESTS

N Fujita received research grants from TOPPAN outside the submitted work. R Katayama received research grants from Chugai, TOPPAN, UBE outside the submitted work. Ethics approval and consent to participate: All animal procedures were performed in accordance with relevant guidelines and regulations, according to the protocol approved by the Committee for the Use and Care of Experimental Animals of JFCR (protocol number: 10-01-22). All patients with OS provided informed consent and agreed to the use of surgically resected specimens for research purposes prior to surgery. The study was conducted in accordance with the Declaration of Helsinki and with the approval of the Institutional Review Board of JFCR (IRB number: 2013-1092).

ADDITIONAL INFORMATION

Supplementary information The online version contains supplementary material available at https://doi.org/10.1038/s41388-024-03251-6.

Correspondence and requests for materials should be addressed to Ryohei Katayama.